

Supplementary Information

Phytantriol and Monoolein in Aqueous Deep Eutectic Solvent and Protic Ionic Liquid Solutions

Karen J Edler¹, Gregory G Warr², Alexander M Djerdjev², Minh Thu Lam², Adrian M Hawley³, Stephen Mudie³

1. Department of Chemistry, University of Bath, Claverton Down, Bath, BA2 7AY, UK. Current address: Centre for Analysis and Synthesis, Department of Chemistry, Lund University, Sweden.
2. School of Chemistry and University of Sydney Nano Institute, The University of Sydney, NSW, 2006, Australia.
3. Australian Synchrotron, ANSTO, 800 Blackburn Road, Clayton, Victoria, 3169, Australia

Contents

Section 1: SAXS Diffraction Data

Figures S1-S5: SAXS diffraction patterns for monoolein in EtAN, EAN, ChCl:U, ChCl:F and ChCl:CA mixtures with water.

Figures S6-S10: SAXS diffraction patterns for phytantriol in EtAN, EAN, ChCl:U, ChCl:F and ChCl:CA mixtures with water.

Section 2: Schematic Isothermal Ternary Phase Diagrams

Figures S11-S12 Schematic isothermal ternary phase diagrams for EtAN and EAN-water with monoolein and phytantriol.

Figures S13-S14 Schematic isothermal ternary phase diagrams for ChCl:U, ChCl:F and ChCl:CA-water mixtures with monoolein and phytantriol.

Figure S15 Schematic binary phase diagram of monoolein (MO) in ChCl:U showing postulated three-phase coexistence condition for low-T Pn3m and high-T HII phases with excess solvent.

Section 3: Properties of the Ionic Liquids and Deep Eutectic Solvents Studied.

Table S1: Physical properties of ChCl:U, ChCl:F, ChCl:CA, EtAN, EAN and water.

1. SAXS Diffraction Data

Figure S1: SAXS diffraction patterns for monoolein in EtAN mixtures with water

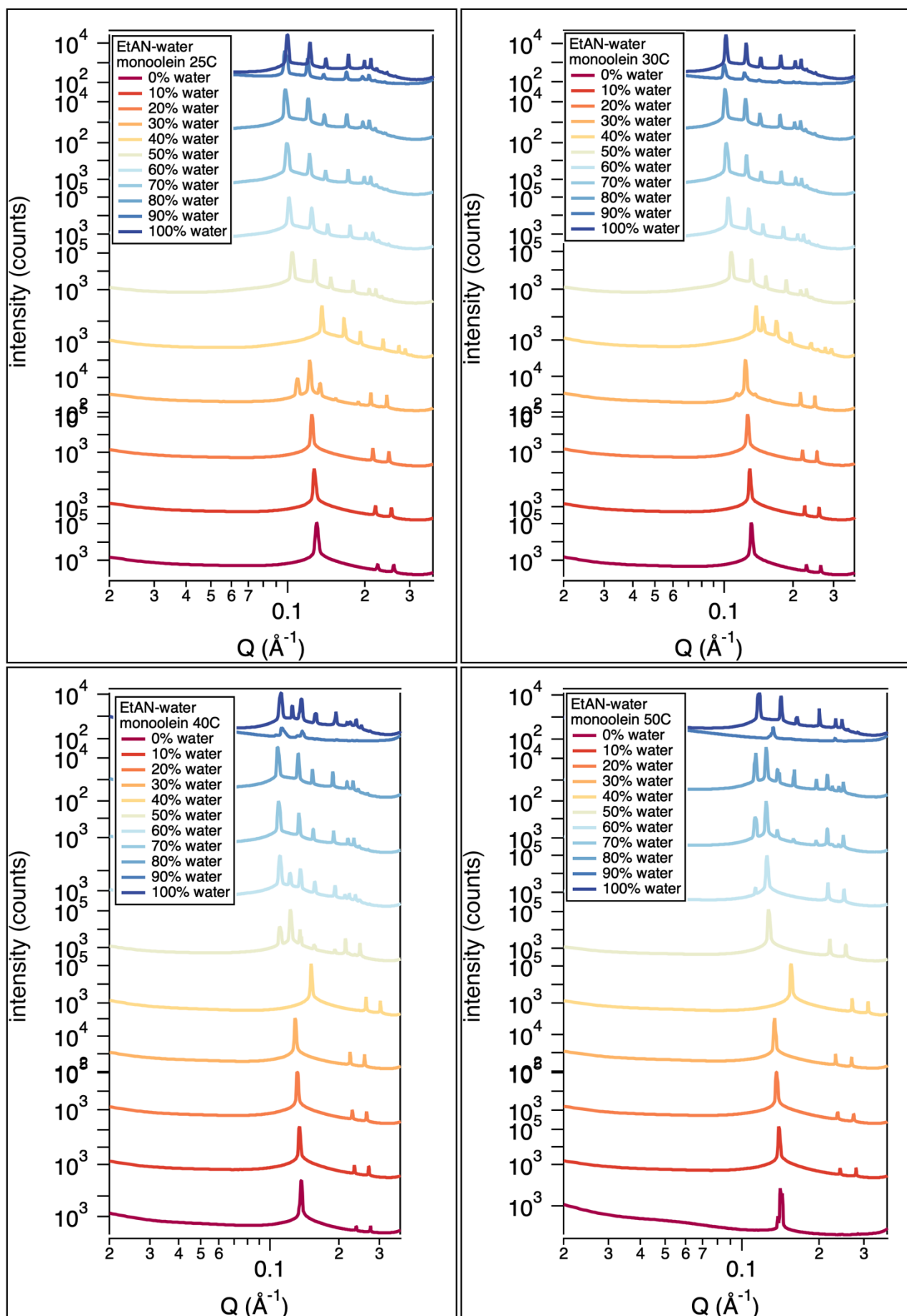


Figure S2: SAXS diffraction patterns for monoolein in EAN mixtures with water.

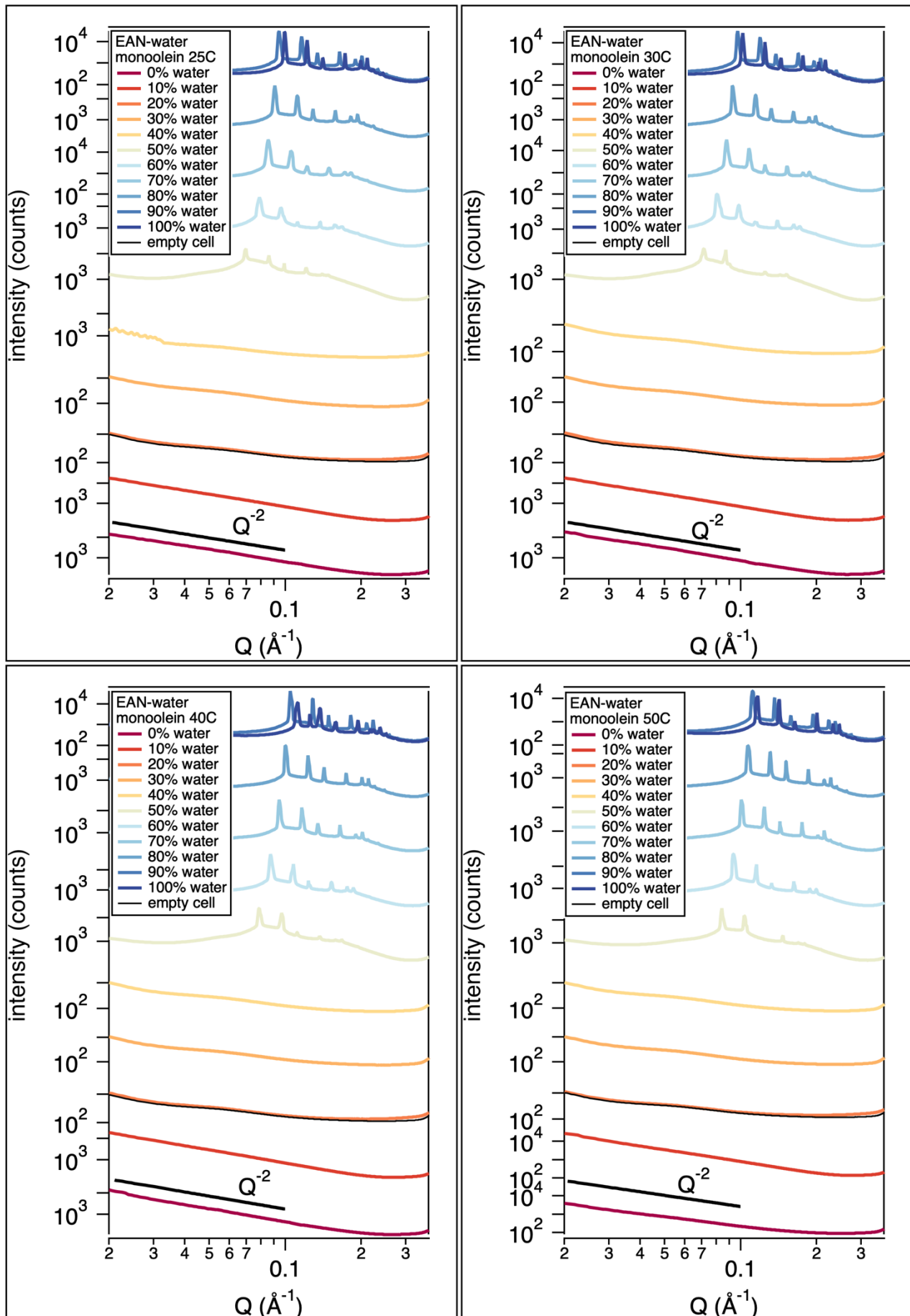


Figure S3: SAXS diffraction patterns for monoolein in ChCl:U mixtures with water.

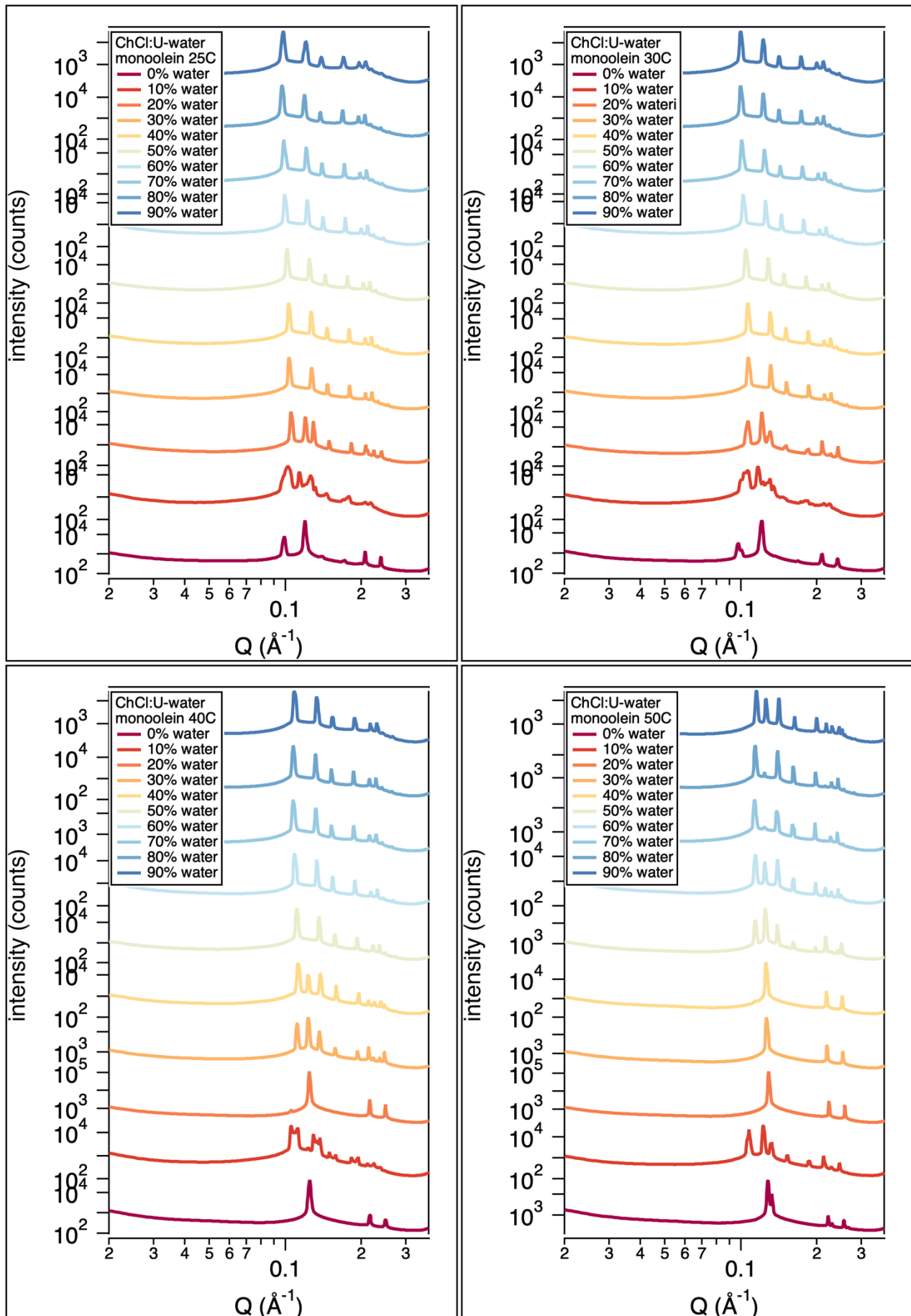


Figure S4: SAXS diffraction patterns for monoolein in ChCl:F mixtures with water.

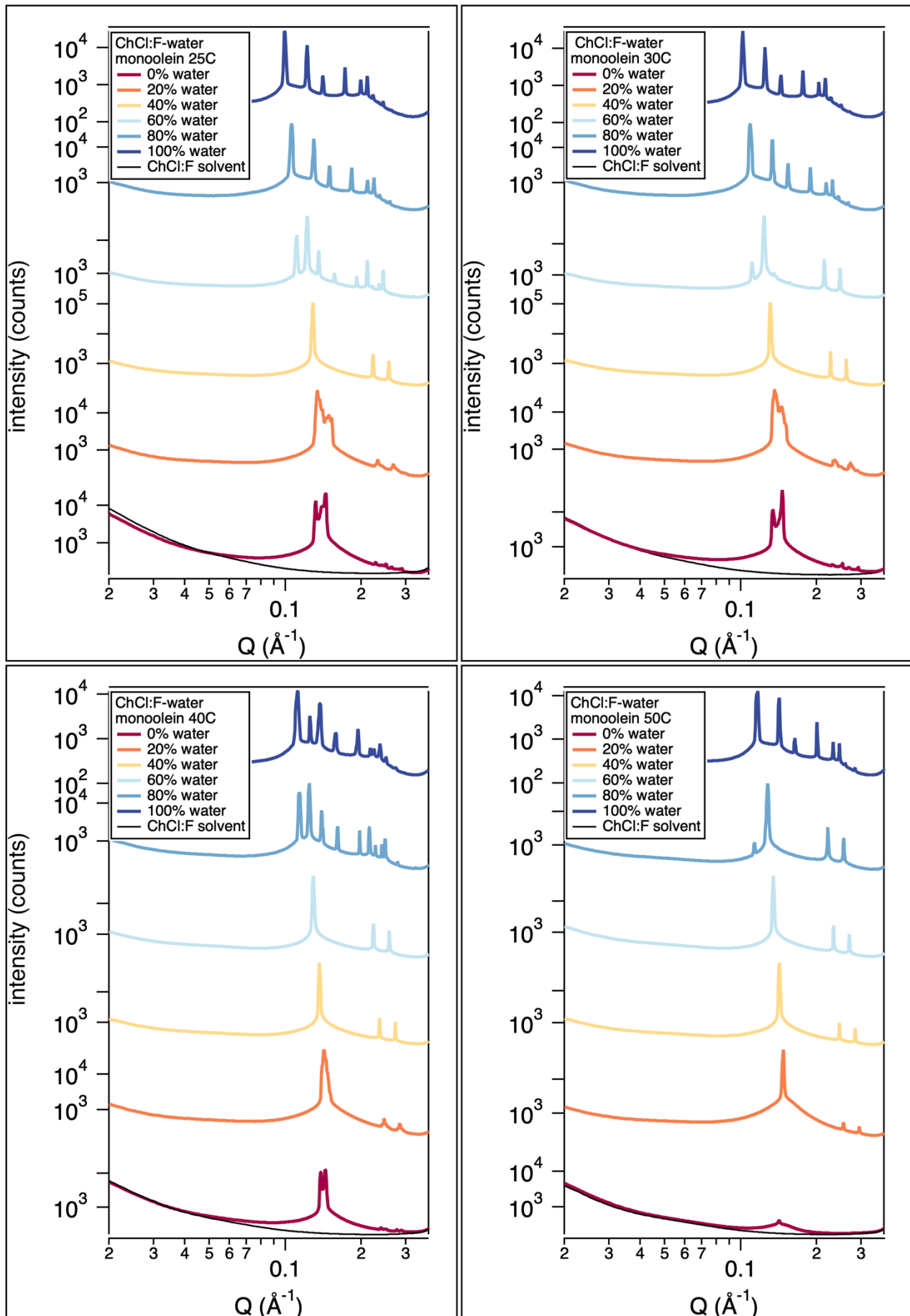


Figure S5: SAXS diffraction patterns for monoolein in ChCl:CA mixtures with water.

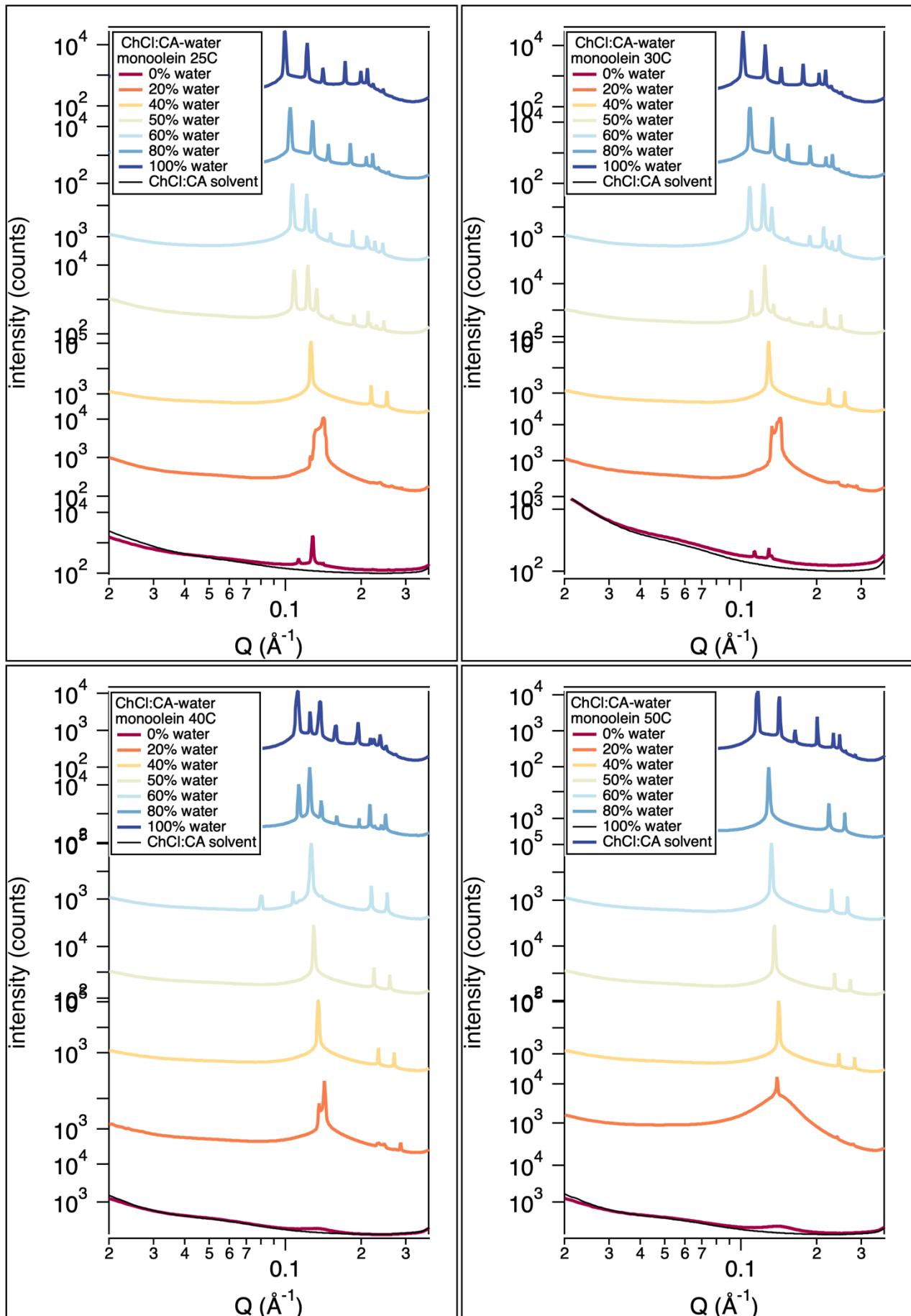


Figure S6: SAXS diffraction patterns for phytantriol in EtAN mixtures with water.

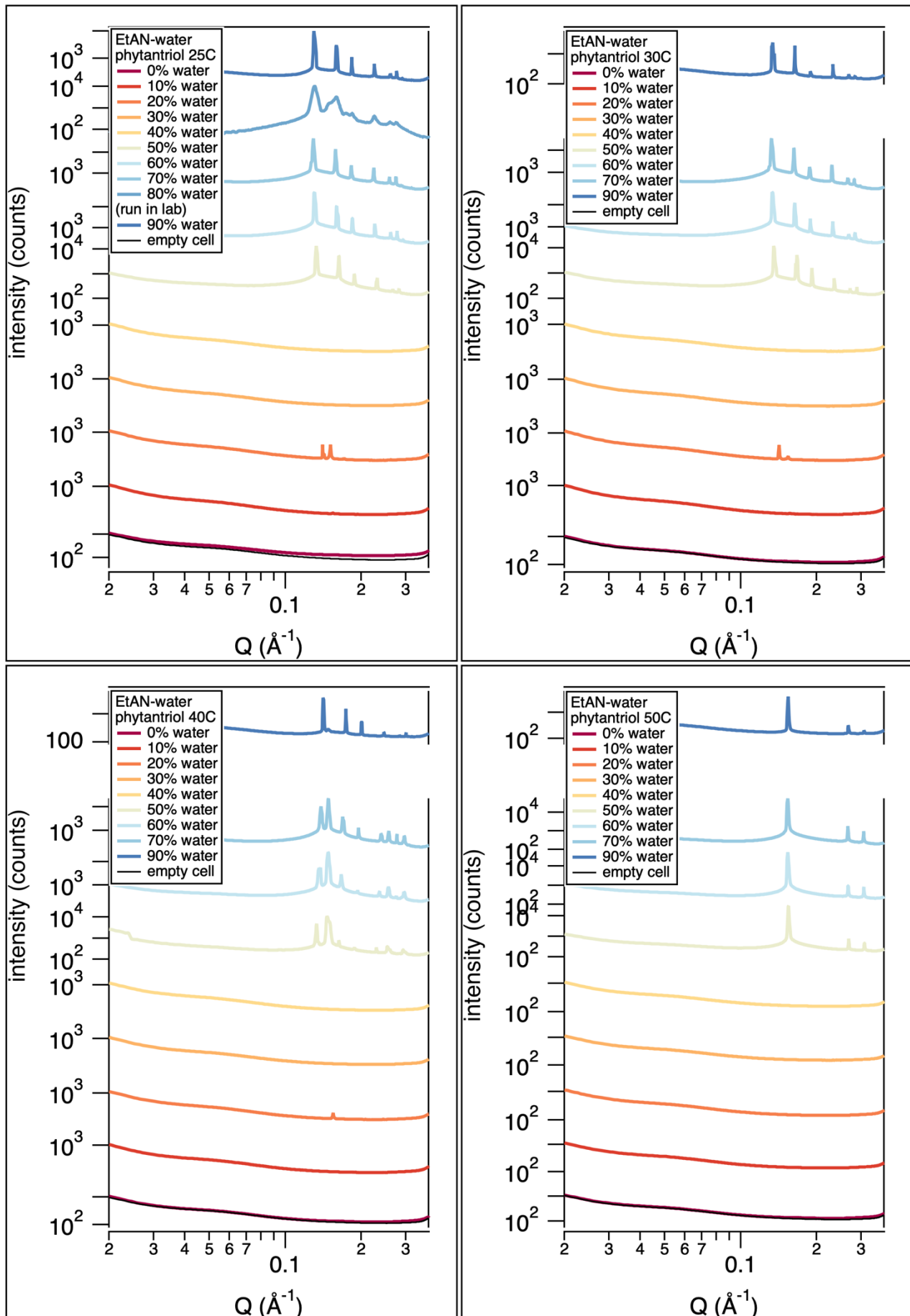


Figure S7: SAXS diffraction patterns for phytantriol in EAN mixtures with water.

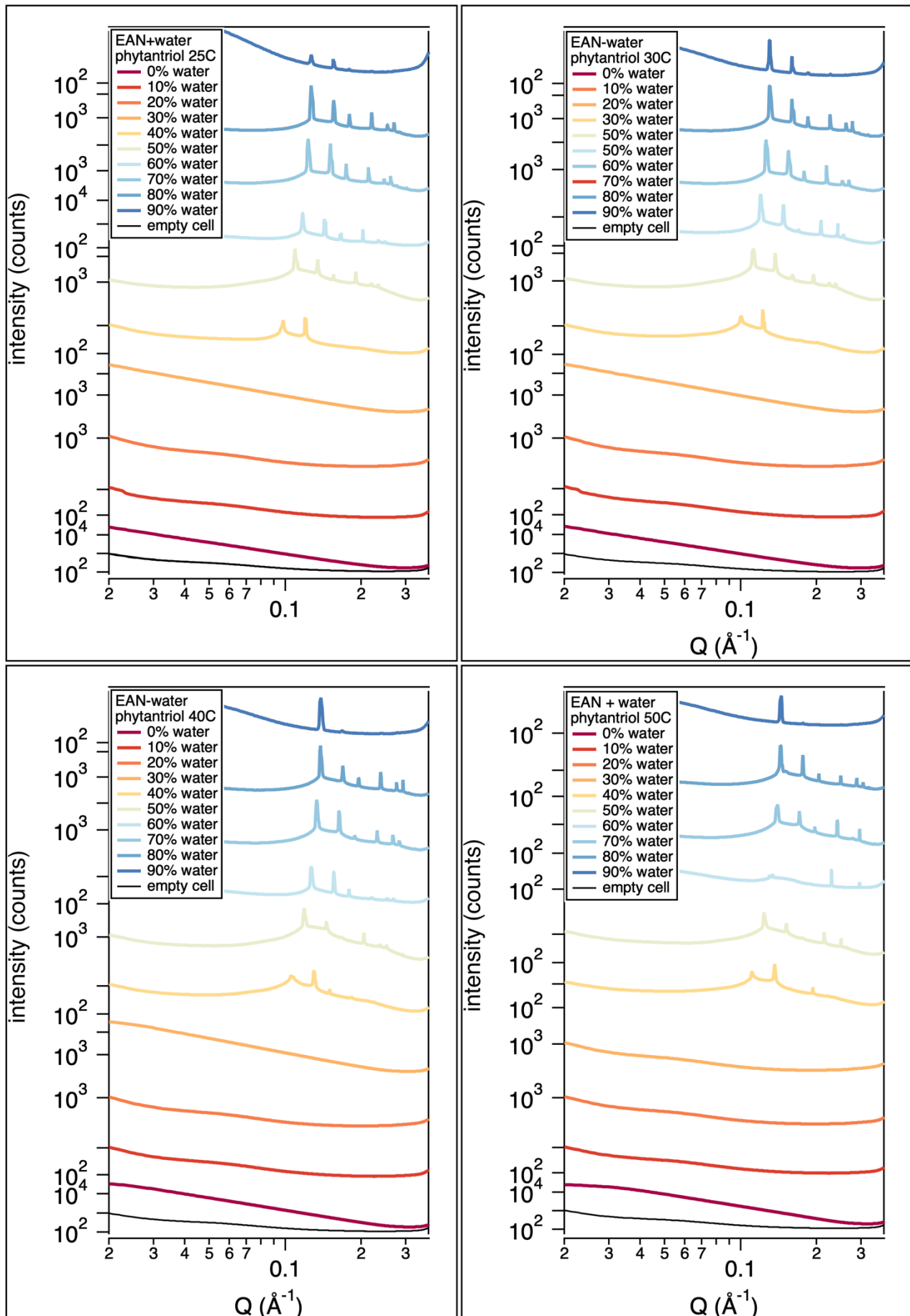


Figure S8: SAXS diffraction patterns for phytantriol in ChCl:U mixtures with water.

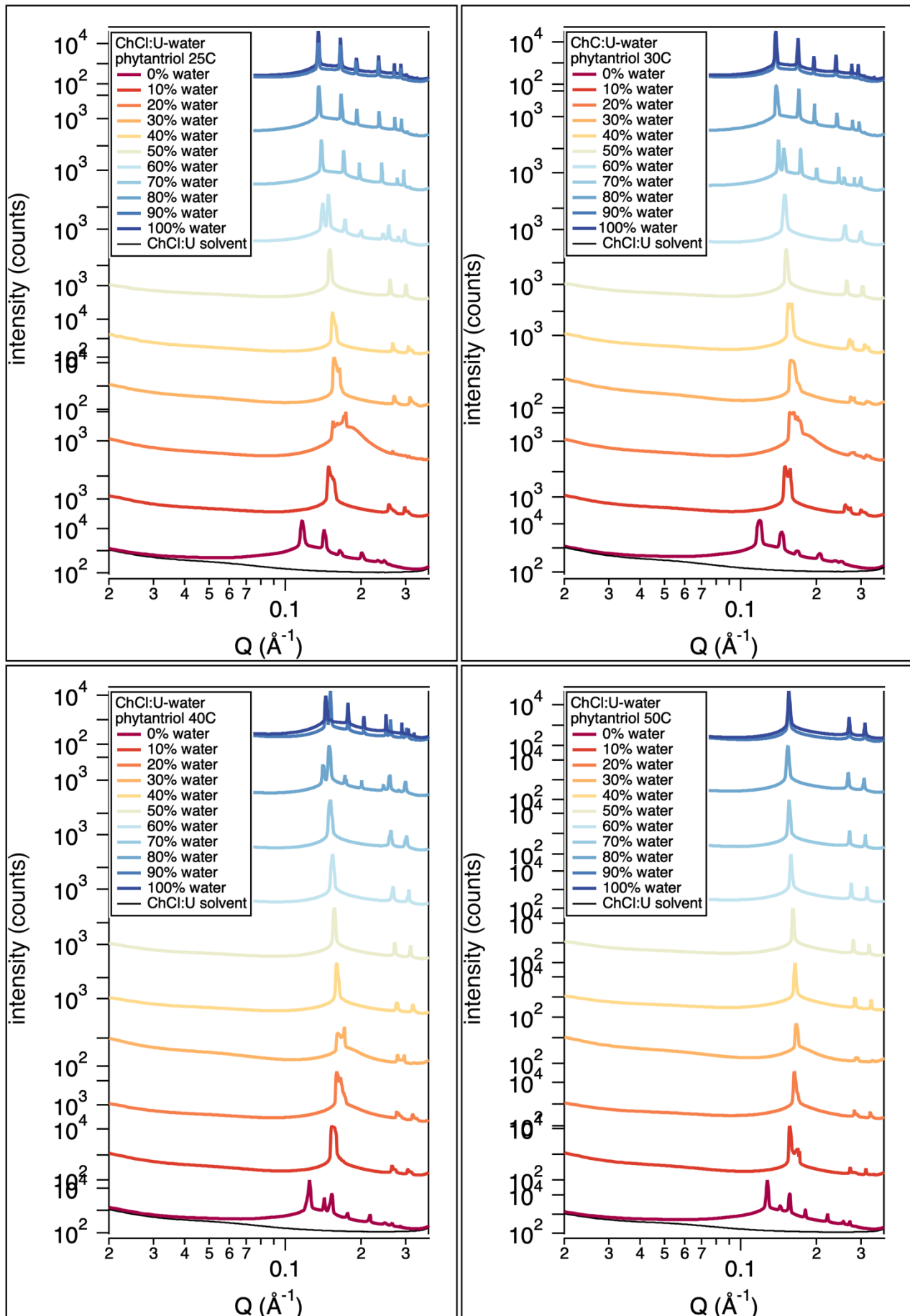


Figure S9: SAXS diffraction patterns for phytantriol in ChCl:F mixtures with water.

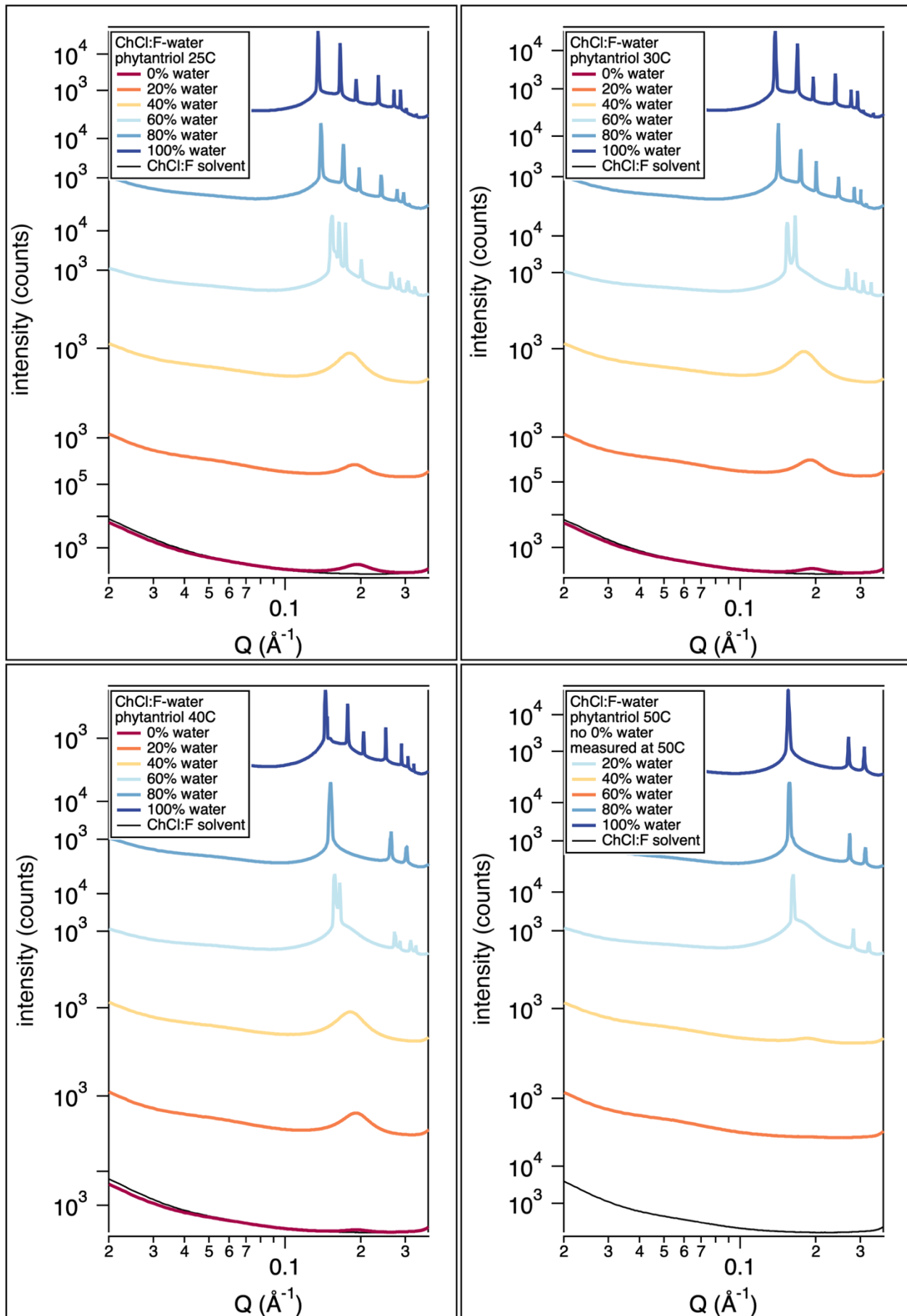
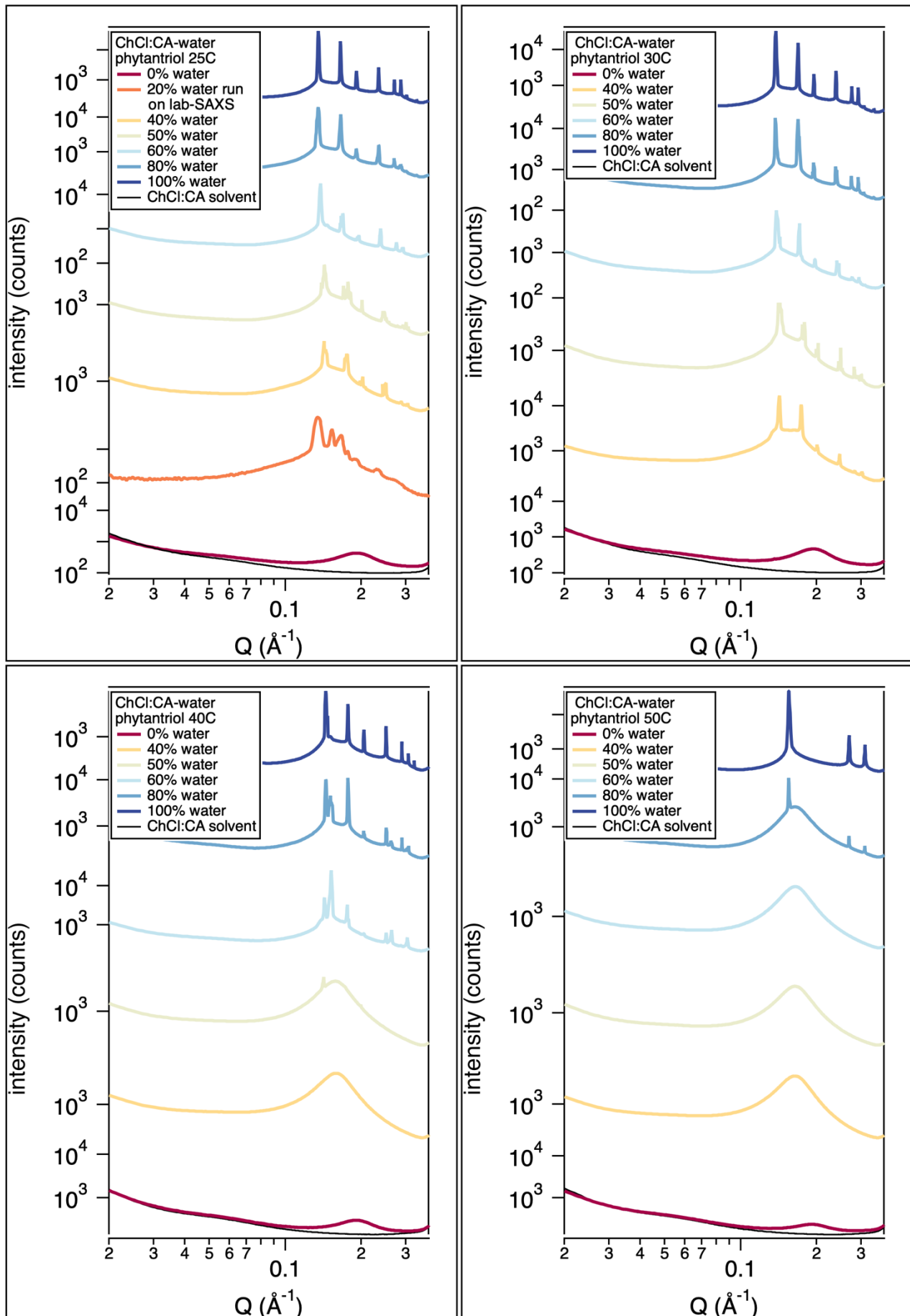


Figure S10: SAXS diffraction patterns for phytantriol in ChCl:CA mixtures with water.



2. Schematic isothermal ternary phase diagrams

Schematic isothermal ternary phase diagrams of lipid/water/solvent systems were drawn based on collected SAXS patterns and macroscopic observations of samples together with available literature phase behaviour in water and for EAN and EtAN with monoolein (Myverol) and phytantriol, and ChCl:U/water/phytantriol. Dashed lines indicate phase boundaries of coexisting lyotropics at maximum swelling, or estimated maximum micelle concentration. Tie lines and tie-triangles indicate approximate 2- and 3-phase coexistence compositions.

Figure S11: Schematic isothermal ternary phase diagrams for monoolein in EtAN-water (top) and EAN-water (bottom) mixtures, drawn combining our data with available literature.

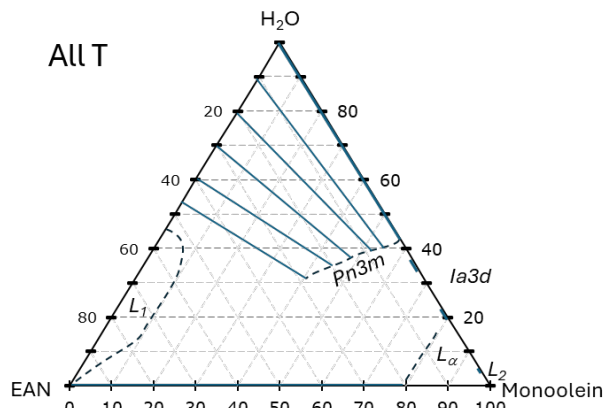
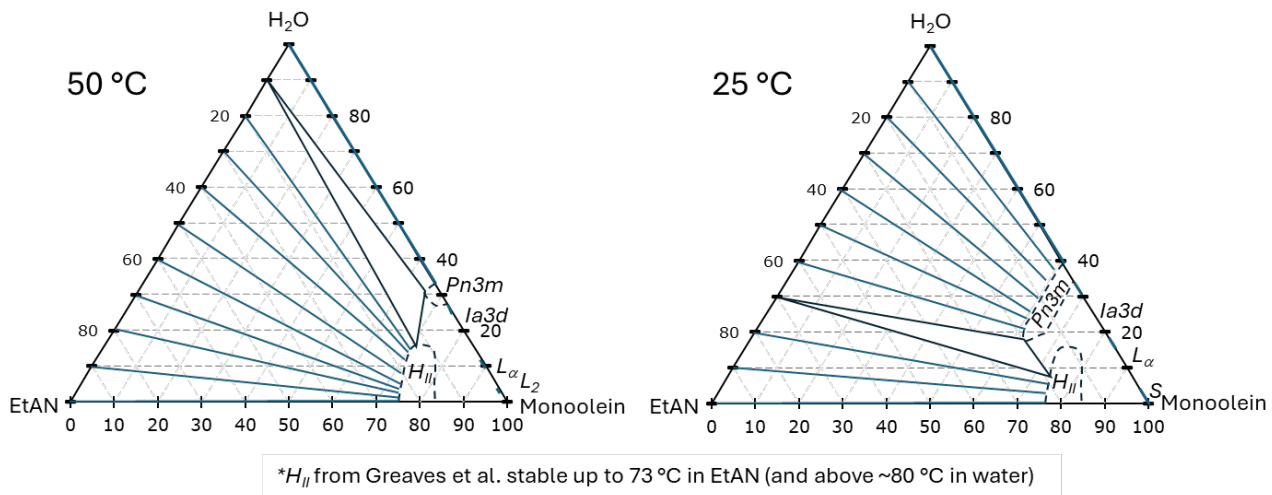


Figure S12: Schematic isothermal ternary phase diagrams for phytantriol in EtAN-water (top) and EAN-water (bottom) mixtures, drawn combining our data with available literature.

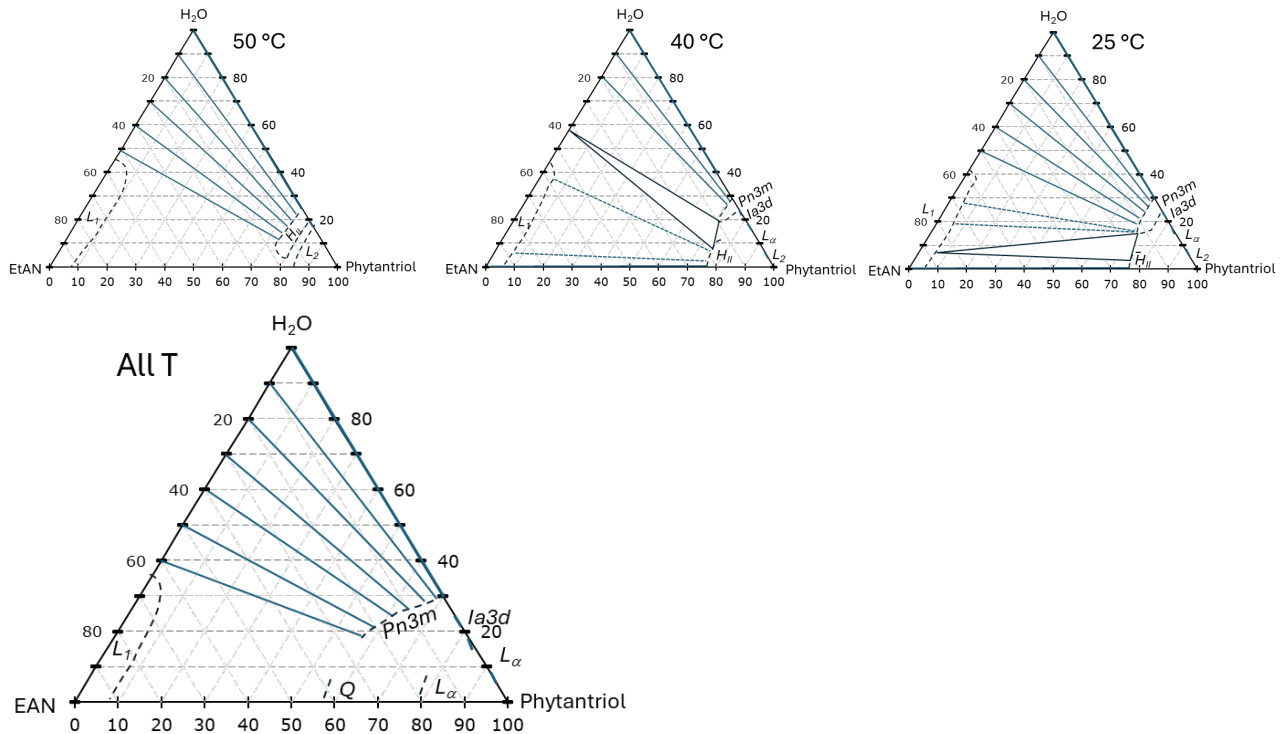


Figure S13: Schematic isothermal ternary phase diagrams for monoolein in ChCl:U-water (top), ChCl:F-water (middle) and ChCl:CA-water (bottom) mixtures, drawn combining our data with available literature.

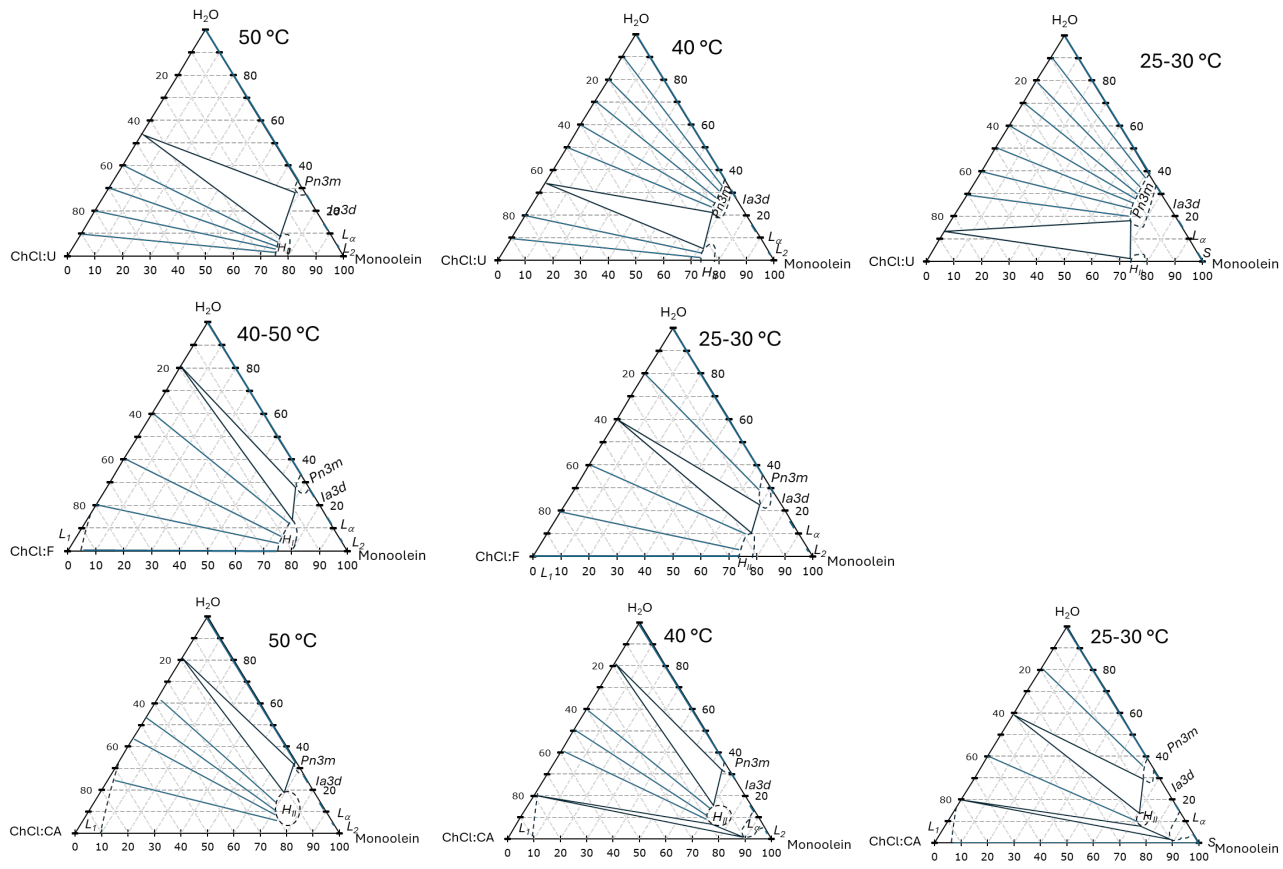
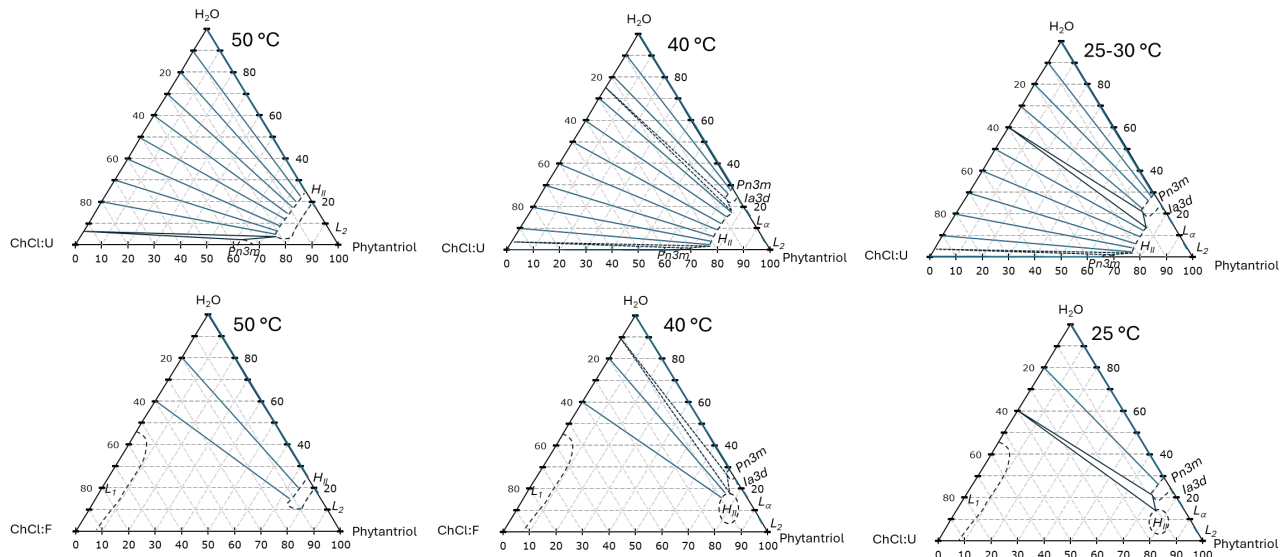


Figure S14: Schematic isothermal ternary phase diagrams for phytantriol in ChCl:U-water (top), ChCl:F-water (middle) and ChCl:CA-water (bottom) mixtures, drawn combining our data with available literature.



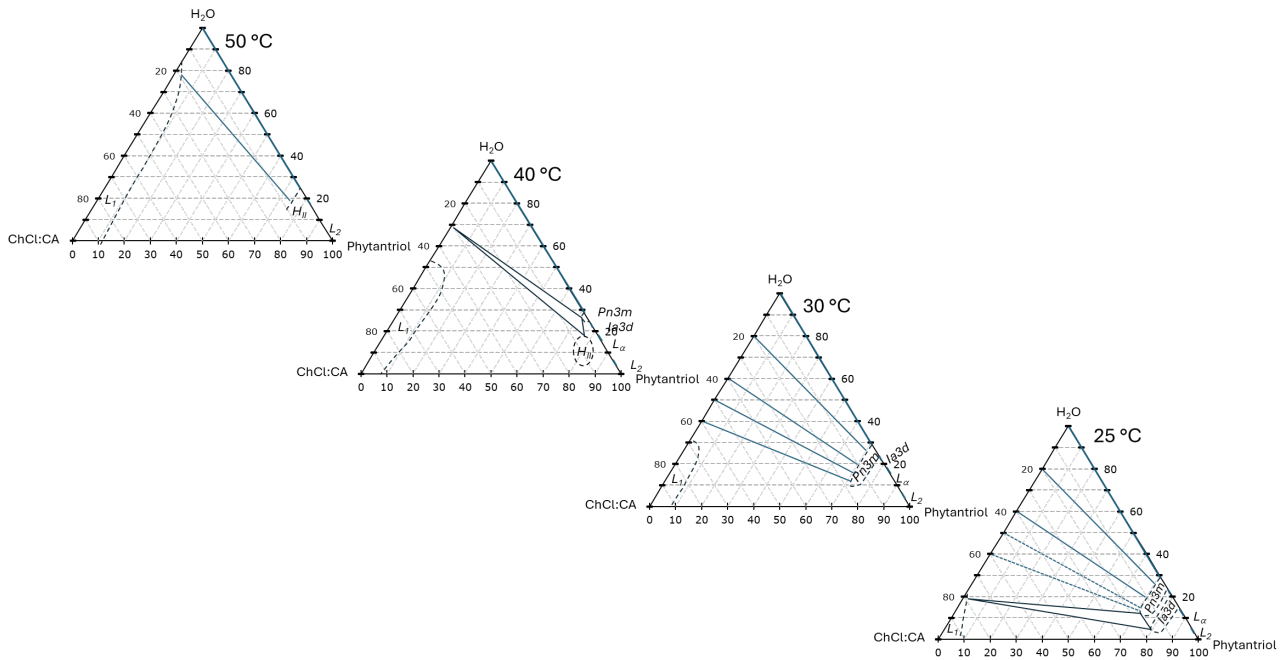
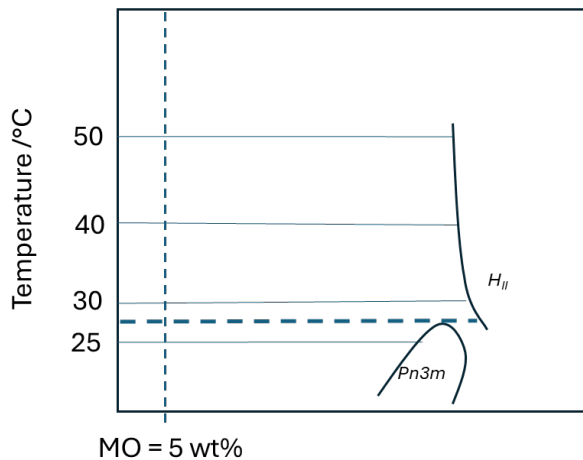


Figure S15. Schematic binary phase diagram of monoolein (MO) in ChCl:U showing postulated three-phase coexistence condition for low-T Pn3m and high-T HII phases with excess solvent.

ChCl:U = 95%



3. Properties of the Ionic Liquids and Deep Eutectic Solvents Studied.

Table S1: Melting point, viscosity, surface tension, Kamlet-Taft parameters (α (HBA acidity), β (HBD basicity), π^* (polarizability)) values from the literature for the solvents used.

| | Melting point | Viscosity / Pa.s | Surface tension /mN m ⁻¹ | α (HBA acidity) | β (HBD basicity) | π^* polarisability |
|---------------|------------------------|--|--|--|--|---|
| ChCl:U (1:2) | 25 °C ¹ | 1.372 (dry, 20°C) ² | 66 ³ | 1.42 ⁴ | 0.50 ⁴ | 1.14 ⁴ |
| ChCl:CA (1:1) | 90.9 °C ⁵ | 10224 (20°C; dry) ⁶ 5233 (20°C; 1wt% water) ⁶ 131 (25°C, 1:1:1 ChCl:CA:H ₂ O 6wt%) ⁷ | 68.59 (1:1:6 ChCl:CA:H ₂ O ie 24.6wt% water) ⁸ | 1.22 (1:1:1 ChCl:CA:H ₂ O ie 6wt% water) ⁹ | Not measurable (1:1:1 ChCl:CA:H ₂ O ie 6wt% water) ⁹ | 1.24 (1:1:1 ChCl:CA:H ₂ O ie 6wt% water) ⁹ |
| ChCl:F (1:1) | 54.47 °C ¹⁰ | 5.587 (dry; 50°C) ¹⁰ 8.696 (25°C, 5.29% water) ¹⁰ | 70.4 ¹¹ | - (dry; not measurable) ¹⁰ 1.13 (9wt% water) ¹⁰ | 0.42 ± 0.04 ¹⁰ 0.53± 0.03 (9wt% water) ¹⁰ | 1.07 ± 0.01 ¹⁰ 1.12 ± 0.02 (9wt% water) ¹⁰ |
| EAN | 12 °C | 0.038 (25°C) ¹² | 48.5 ¹³ | 1.09 ±0.04 ¹⁴ | 0.55±0.04 ¹⁴ | 1.08±0.02 ¹⁴ |
| EtAN | 52-53 °C ¹⁵ | 0.113 (25°C) ¹⁶ | 72.1 ¹³ | 1.10±0.04 ¹⁴ | 0.45±0.04 ¹⁴ | 1.17±0.02 ¹⁴ |
| water | 0 °C | 0.001 | 72.8 | 1.17 ¹⁷ | 0.14 ¹⁷ | 1.09 ¹⁷ |

References:

1. X. Meng, K. Ballerat-Busserolles, P. Husson and J.-M. Andanson, *New J. Chem.*, 2016, **40**, 4492-4499
2. A. Yadav and S. Pandey, *Journal of Chemical & Engineering Data*, 2014, **59**, 2221-2229.
3. T. Arnold, A. J. Jackson, A. Sanchez-Fernandez, D. Magnone, A. E. Terry and K. J. Edler, *Langmuir*, 2015, **31**, 12894-12902.
4. C. Florindo, A. J. S. McIntosh, T. Welton, L. C. Branco and I. M. Marrucho, *Physical Chemistry Chemical Physics*, 2018, **20**, 206-213.
5. E. A. Crespo, L. P. Silva, M. A. R. Martins, M. Bülow, O. Ferreira, G. Sadowski, C. Held, S. P. Pinho and J. A. P. Coutinho, *Ind. Eng. Chem. Res.*, 2018, **57**, 11195-11209.
6. I. M. Aroso, A. Paiva, R. L. Reis and A. R. C. Duarte, *Journal of Molecular Liquids*, 2017, **241**, 654-661.
7. M. H. Shafie, R. Yusof and C.-Y. Gan, *J. Mol. Liq.*, 2019, **288**, 111081.
8. N. López, I. Delso, D. Matute, C. Lafuente and M. Artal, *Food Chemistry*, 2020, **306**, 125610.

9. E. Husanu, A. Mero, J. G. Rivera, A. Mezzetta, J. C. Ruiz, F. D'Andrea, C. S. Pomelli and L. Guazzelli, *ACS Sustainable Chemistry & Engineering*, 2020, **8**, 18386-18399.
10. L. P. Silva, L. Fernandez, J. H. F. Conceição, M. A. R. Martins, A. Sosa, J. Ortega, S. P. Pinho and J. A. P. Coutinho, *ACS Sus. Chem. Eng.*, 2018, **6**, 10724-10734.
11. A. Hayyan, F. S. Mjalli, I. M. AlNashef, T. Al-Wahaibi, Y. M. Al-Wahaibi and M. A. Hashim, *Thermochimica Acta*, 2012, **541**, 70-75.
12. D. Ausín, J. J. Parajó, J. L. Trenzado, L. M. Varela, O. Cabeza and L. Segade, *International Journal of Molecular Sciences*, 2021, **22**, 7334.
13. D. Wakeham, D. Eschebach, G. B. Webber, R. Atkin and G. G. Warr, *Australian Journal of Chemistry*, 2012, **65**, 1554-1556.
14. D. Yalcin, C. J. Drummond and T. L. Greaves, *Physical Chemistry Chemical Physics*, 2020, **22**, 114-128.
15. T. L. Greaves and C. J. Drummond, *Chemical Reviews*, 2008, **108**, 206-237.
16. T. L. Greaves, A. Weerawardena, C. Fong, I. Krodkiewska and C. J. Drummond, *J. Phys. Chem. B*, 2006, **110**, 22479-22487.
17. P. G. Jessop, D. A. Jessop, D. Fu and L. Phan, *Green Chemistry*, 2012, **14**, 1245-1259.